Oncogene (2006) 25, 1841–1851

www.nature.com/onc

ORIGINAL ARTICLE

Smad4 haploinsufficiency in mouse models for intestinal cancer

P Alberici[1], S Jagmohan-Changur[2], E De Pater[1], M Van Der Valk[3], R Smits[1], P Hohenstein[4] and R Fodde[1]

[1]*Department of Pathology, Josephine Nefkens Institute, ErasmusMC, Rotterdam, The Netherlands;* [2]*Center for Human and Clinical Genetics, Leiden University Medical Center, Leiden, The Netherlands;* [3]*Department of Experimental Animal Pathology, Netherlands Cancer Institute, Amsterdam, The Netherlands and* [4]*MRC Human Genetics Unit, Edinburgh, UK*

The *Smad4*$^{+/E6sad}$ mouse carries a *null* mutation in the endogenous *Smad4* gene resulting in serrated adenomas and mixed polyposis of the upper gastrointestinal (GI) tract with 100% penetrance. Here, we show by loss of heterozygosity (LOH) analysis and immunohistochemistry (IHC) that, although the majority of the tumors appear at 9 months of age, somatic loss of the wild-type *Smad4* allele occurs only at later stages of tumor progression. Hence, haploinsufficiency underlies *Smad4*-driven tumor initiation in the GI tract. As both the *Apc* and *Smad4* tumor suppressor genes map to mouse chromosome 18, we have bred *Smad4*$^{+/E6sad}$ with the *Apc*$^{+/1638N}$ model to generate two distinct compound heterozygous lines carrying both mutations either *in cis* (CAS) or *in trans* (TAS). Strikingly, both models show increased tumor multiplicities when compared with the single mutant littermates, although CAS mice are more severely affected and became moribund at only 5–6 weeks of age. Phenotypic and molecular analyses indicate that *Smad4* haploinsufficiency is sufficient to significantly affect tumor initiation and progression both prior to and upon loss of Apc function. Moreover, complete loss of Smad4 strongly enhances *Apc*-driven tumor formation.
Oncogene (2006) **25,** 1841–1851. doi:10.1038/sj.onc.1209226; published online 14 November 2005

Keywords: Smad4; Apc; haploinsufficiency; TGF-β signaling; LOH; Wnt signaling; gastrointestinal cancer

Introduction

Loss of heterozygosity (LOH) and point mutations at the *SMAD4*/*DPC4* tumor suppressor gene, a key signal transducer in the TGF-β and BMP signaling pathways, are usually found at late stages of sporadic colorectal cancer (CRC) (Takagi *et al*., 1996; Thiagalingam *et al*., 1996; Koyama *et al*., 1999). In the classical adenoma-carcinoma progression sequence originally proposed for CRC by Fearon and Vogelstein, loss of *APC* function triggers tumor initiation, followed by constitutional activation of the *KRAS* oncogene during adenoma progression, and by loss and mutation of the *SMAD2*/*4* and *TP53* tumor suppressors at chromosome 18p and 17q, respectively, at more advanced stages of adenoma growth and malignant transformation (Fearon and Vogelstein, 1990). On the other hand, germline mutations of the *SMAD4* gene are responsible for a subset of familial Juvenile Polyposis (JP), an autosomal dominant predisposition to the development of multiple hamartomatous polyps and GI cancer (Howe *et al*., 1998).

In order to elucidate the role played by *SMAD4* in intestinal tumor initiation and progression, several mouse models have been generated that carry targeted inactivating mutations in the endogenous mouse *Smad4* gene (Sirard *et al*., 1998; Takaku *et al*., 1999; Xu *et al*., 2000). In all cases, homozygosity for the *Smad4* mutation results in embryonic lethality prior to E9.5 due to defects in gastrulation and mesodermal development. Heterozygous *Smad4*$^{+/-}$ mice develop gastric and duodenal tumors with features reminiscent of human juvenile polyps. Notably, Xu and co-workers detected LOH at the *Smad4* locus only at late stages of tumor progression, namely in large dysplastic polypous tumors.

More recently, our laboratory has reported the *Sad* (*Smad4*^{E6sad}) mouse model, characterized by a *null* mutation of the mouse *Smad4* gene, namely a single-nucleotide deletion in the exon 6 splice acceptor site resulting in an unstable mRNA and undetectable levels of the Smad4 protein (Hohenstein *et al*., 2003). Older F1 (129Ola $\times$ C57BL/6) *Smad4*$^{+/E6sad}$ animals are predisposed to late-onset (18 months) serrated adenomas and mixed adenomatous and hyperplastic polyps, mainly localized immediately distal to the pyloric/duodenal transitional area. In our original report, LOH of the wild-type *Smad4* gene could only be assessed in mice older than 18 months and it was found in the majority of tumors collected from *Smad4*$^{+/E6sad}$ mice. To address the issue of haploinsuffciency in *Smad4*-driven intestinal tumorigenesis, we now have closely monitored inbred C57BL/6J (F5-F8 backcross generation) *Smad4*$^{+/E6sad}$ mice at different ages, from 6 to 18 months, to evaluate the onset of the tumor formation and of *Smad4* LOH during tumor initiation and progression.

Correspondence: Professor R Fodde, Department of Pathology, ErasmusMC, PO Box 1738, 3000 DR Rotterdam, The Netherlands.
E-mail: r.fodde@erasmusmc.nl
Received 6 June 2005; revised 11 August 2005; accepted 29 September 2005; published online 14 November 2005

Furthermore, to examine the role of *Smad4* status in *Apc*-driven intestinal tumorigenesis, we bred the *Smad4*^{E6sad} mutation with the *Apc*$^{+/1638N}$ model, previously developed and characterized in our laboratory (Fodde *et al*., 1994). As both *Apc* and *Smad4* map to mouse chromosome 18, two different *Apc*$^{+/1638N}$/*Smad4*$^{+/E6sad}$ compound heterozygous models were generated, in *trans* (mutations on different chromosomes) and, by meiotic recombination, *in cis* (mutations on the same chromosome).

Phenotypic and tumor analysis of the compound *Apc*$^{+/1638N}$/*Smad4*$^{+/E6sad}$ mice indicates a differential role for *Smad4* in combination with the mutated *Apc* in intestinal tumor initiation and progression.

Results

GI tumor incidence, distribution, and histopathology in Smad4$^{+/E6sad}$ *mice*

We previously described the identification and initial characterization of the *Smad4*$^{+/E6sad}$ mouse model (Hohenstein *et al*., 2003), characterized by hyperplastic and serrated adenomas resulting from a germline *null* mutation at the endogenous *Smad4* gene. To provide a more detailed characterization of their phenotype and pattern of GI tumor initiation and progression in a genetic background comparable to the other described models (Sirard *et al*., 1998; Takaku *et al*., 1999; Xu *et al*., 2000), *Smad4*$^{+/E6sad}$ mice were backcrossed for 5–8 generations to C57BL/6JIco and analysed at the age of 6, 9, 12, 15 and 18 months. For each time point, at least nine mice of both genders were analysed. Microscopic examination of the GI-tract in 6-month-old mice did not reveal any neoplastic lesions, thus confirming the late-onset nature of the tumor phenotype in this model (not shown). However, already at 9 months, 100% of the *Smad4*$^{+/E6sad}$ mice analysed revealed the presence of polyps in the stomach (fundus) (Table 1). At the same age, tumors were also found in the peri-ampullary region in approximately 50% of *Smad4*$^{+/E6sad}$ mice. At age 12 months and older, the latter proportion increases up to 80–100% of the animals, while a subset (3/11, 27% at 12 months; 3/10, 30% at 15 months; 6/9, 66% at 18 months) showed carpeting (here defined as an area where an extremely high polyp density did not allow counting) of the whole pyloric/duodenal transition area with polyps.

Additional tumors were found throughout the rest of the small intestinal tract (duodenum, jejunum, and ileum) starting from age 9 months, whereas colorectal polyps were only found in few animals at later stages (1/10, 10% at 15 months; 2/9, 22% at 18 months). The average number of gastric polyps per mouse did not increase over time though a slight increase in gastric tumor size was observed (from 3 mm $\pm$ 1 at 9 months up to 8 mm $\pm$ 2 at 18 months). The number of polyps present throughout the entire intestinal tract clearly increased over time, from an average of 3 at 9 months to 9 at 18 months of age. Analysis of these tumors by histopathology confirmed previously observed features: polyps were hyperplastic with branching villi (Figure 1a) and occasionally with serrated aspects. In the more advanced cases, dilated cysts and foci of frank dysplasia with increased nuclear cytoplasmic ratio and nuclear stratification of the cells were present (Figure 1b). Macroscopic examination of >1-year-old *Smad4*$^{+/E6sad}$ animals did not reveal the presence of tumors in other tissues/organs including the pancreas.

Haploinsufficiency at the Smad4 *gene in GI tumors from* Smad4$^{+/E6sad}$ *mice*

To investigate the role of LOH as a tumor-initiating event in the *Smad4*$^{+/E6sad}$ mouse model, a total of 50 tumors and normal controls were analysed both by DNA- and protein-based methods. To enrich in tumor DNA, DNA samples were isolated from tumor cells obtained by laser capture microdissection (LCM) of histological sections. For each age group, from 9 to 18 months of age, at least 10 tumors and two normal intestinal tissue controls, were microdissected by LCM for DNA isolation. LOH of the wild-type *Smad4* allele was established using two CA repeat markers, *d18Mit81* and *d18Mit80*, located, respectively, 7 cM proximal and 2 cM distal to the *Smad4* gene on chromosome 18, as previously described (Hohenstein *et al*., 2003).

LOH of the *Smad4* allele was not detected in polyps from *Smad4*$^{+/E6sad}$ mice up to 15 months (Table 2). At

Table 1 Incidence and distribution of intestinal neoplasia in *Smad4*^{E6sad} mice at different time points

No. of mice	*Age (months)*	*Incidence (%)*	*Tumor multiplicity/ animal*	*Tumor range*	*Histology*	*Tumor localization*
9	6	0	—	—	—	—
10	9	100	3	2–5	Hyperplastic polyps	S: 100%; P: 50%; D: 10%; J: 30%; I: 0%; C:0%
10	12	100	5	2–7	Hyperplastic polyps	S: 100%; P: 80%; D: 10%; J: 0%; I: 10%; C: 0%
10	15	100	7	4–12	Low dysplastic polyps	S: 100%; P: 100%; D: 20%; J: 20%; I: 40%; C: 10%
9	18	100	9	3–13	Low dysplastic polyps	S: 100%; P: 100%; D: 10%; J:10%; I: 11%; C: 22%

Tumor localization: incidence of one or more lesions in the corresponding part of the intestinal tract: S = stomach, P = periampullar region, D = duodenum, J = jejunum, I = ileum, C = colon.

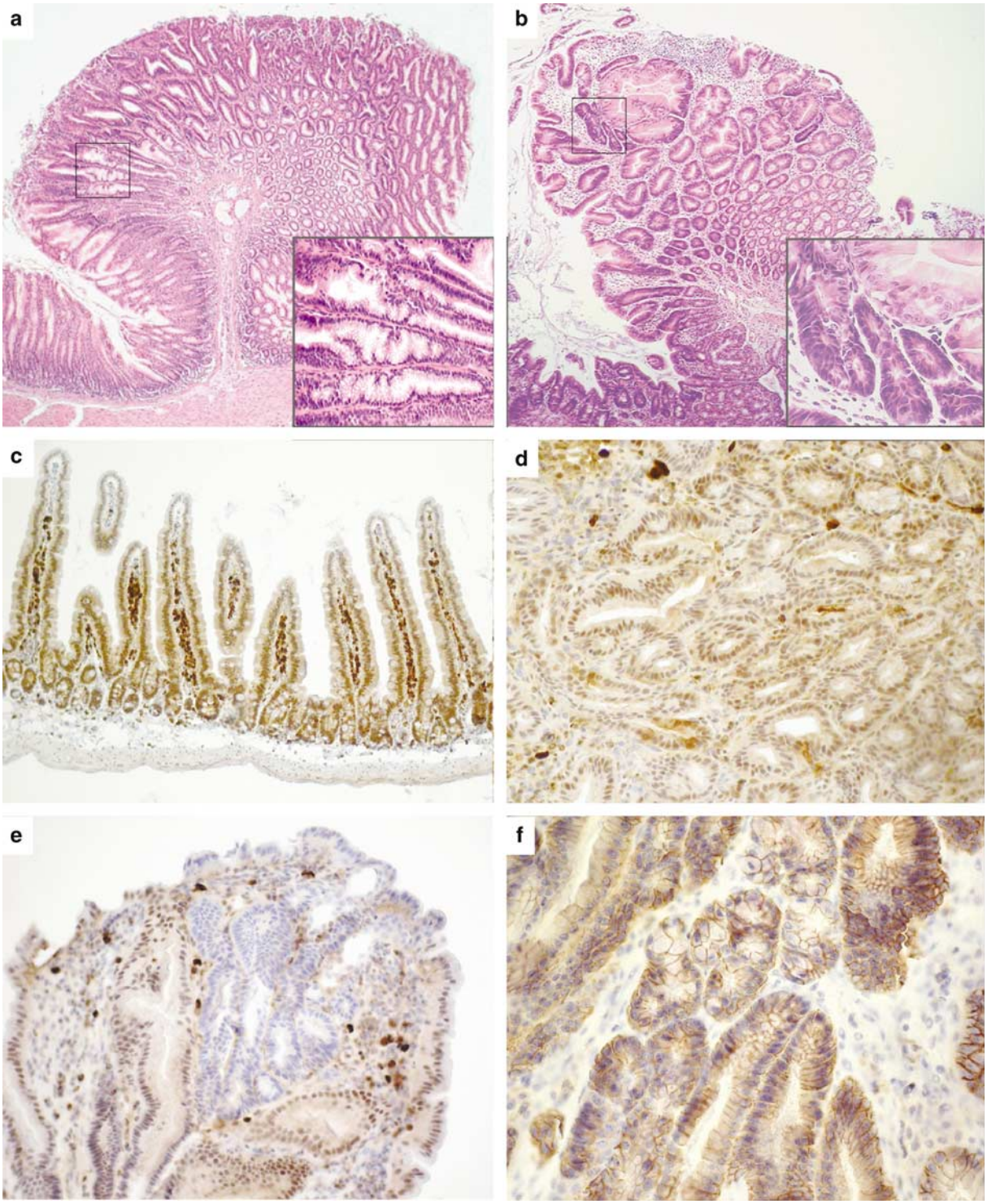

Figure 1 Histopathology and immunohistochemical analysis of *Smad4*^{E6sad} small intestinal polyps at different ages and progression stages. (**a**) Polyp originated in the gastric epithelium from a 12-month- old *Smad4*$^{+/E6sad}$ animal. Inset: higher magnification of a hyperplastic region. Note the gastric epithelium (HE). (**b**) Advanced polyp from a 15-month-old *Smad4*$^{+/E6sad}$ mouse showing areas of frank dysplasia. Inset: higher magnification of a dysplastic region (HE). (**c**) Smad4 IHC analysis of normal small intestinal epithelium from an *Smad4*$^{+/E6sad}$ animal shows nuclear and cytoplasmatic staining with a crypt-villus decreasing gradient of expression. The aspecific staining in the lamina propria is due to mouse IgG cross-reaction from the secondary antibody. (**d**) Smad4 IHC analysis of a tumor from a 12-month-old *Smad4*$^{+/E6sad}$ mouse shows positive staining of tumor cells. Staining of stromal cells is due to mouse IgG cross-reaction from the secondary antibody. (**e**) Smad4 IHC analysis of a tumor from a 15-month-old *Smad4*$^{+/E6sad}$ mouse shows an area of negatively stained parenchymal cells within an otherwise positive tumor. (**f**) β-Catenin IHC analysis of a tumor from a 15-month-old *Smad4*$^{+/E6sad}$ animal. The more dysplastic area of the lesion mainly shows membranous staining.

Table 2 LOH and IHC analysis of *Smad4*^{E6sad} intestinal tumors

Age (months)	*No. of tumors*	*LOH incidence*	*IHC staining*
6	NA	NA	NA
9	10	0/10 (0%)	+
12	10	0/10 (0%)	+
15	10	4/10 (40%)	− (patchy)
18	14	9/14 (64%)	− (patchy)

NA, not applicable.

this age, four out of 10 (40%) tumors showed LOH. In older mice (18 months), the fraction of tumors presenting LOH at the *Smad4* locus increases (9/14: 64%) in accordance with our own previously published results obtained with mice older than 18 months (Hohenstein *et al*., 2003).

In the majority of the cases ($n = 10/10$ LOH negative and $n = 7/10$ LOH positive), the above data could be confirmed by direct sequence analysis of the *Smad4* gene amplified by PCR from tumor DNA samples. The frameshift visible in the chromatogram of an *Smad4*$^{+/E6sad}$ normal mucosa control sample and due to a single-nucleotide (A) deletion in the exon 6 splice acceptor site of the mutated allele, is lost or clearly reduced in the tumor samples previously shown by CA repeat markers to carry LOH at the *Smad4* locus (Figures 2b and c).

To further confirm the observed haploinsuffciency and late-onset LOH in *Smad4*^{E6sad} GI tumors, we performed immunohistochemistry (IHC) on tumor sections with a Smad4-specific antibody (B-8; see Material and methods) (Wilentz *et al*., 2000; Salovaara *et al*., 2002). Normal gastric and small intestinal mucosa displayed positive staining for Smad4 in all cases, although the intensity of expression was reduced in gastric mucosa when compared to the intestinal epithelium. In the latter, a gradient of expression was observed along the crypt-villus axis, with strong positive nuclei in the crypt, and cytoplasmic staining in the apical part of the villus, similar to the pattern reported by Salovaara *et al*. (2002) in normal human colonic mucosa (Figure 1c).

Tumors derived from *Smad4*$^{+/E6sad}$ mice up to 12 months of age showed in all cases ($n = 4$) positive staining for the protein (Figure 1d). Only in few tumors collected at 14 and 15 months of age (1/6 and 2/5, respectively), loss of Smad4 protein expression was detected in a 'patchy', heterogeneous pattern: Smad4-negative foci were scattered among otherwise positive tumor cells (Figure 1e) (Table 2).

Overall, the results of our LOH and IHC analyses of GI tumors from *Smad4*$^{+/E6sad}$ mice at different ages are consistent with the idea that complete loss of Smad4 function is a late event in tumor progression.

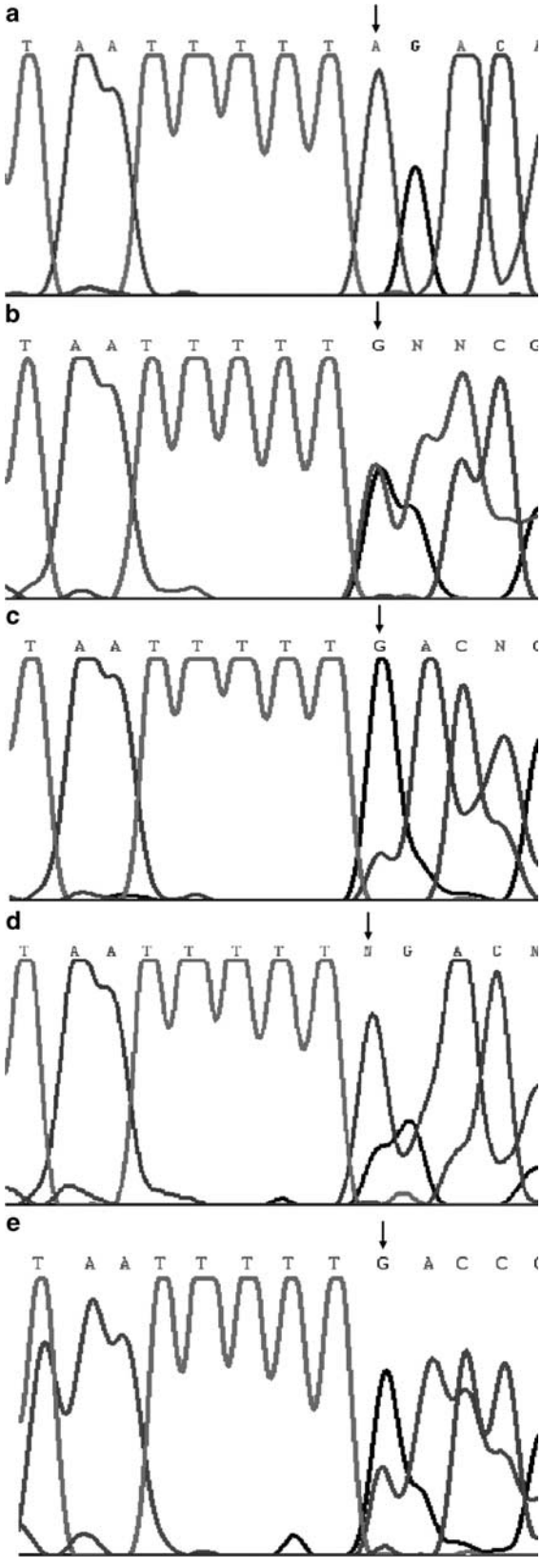

Figure 2 LOH analysis by direct sequencing of the *Smad4* intron 5–exon 6 boundary from tumor and normal DNA samples. The arrow indicates the nucleotide position (A) deleted in the *Smad4*^{E6sad} allele. (**a**) Wild-type sequence from normal intestinal epithelium. (**b**) Heterozygous sequence from a normal mucosa of a *Smad4*$^{+/E6sad}$ mouse. (**c**) Loss of the wild-type *Smad4* allele in intestinal tumor from an 18-month-old *Smad4*$^{+/E6sad}$ mouse. (**d**) Loss of the *Smad4*^{E6sad} allele in a TAS tumor. (**e**) Loss of the wild-type *Smad4* allele in a CAS tumor.

Table 3 Incidence and distribution of intestinal tumors in $Apc^{1638N}/Smad4^{E6sad}$ compound TAS and CAS mice and their single transgenic littermates

Genotype	*No. of mice*	*Median age (range)*	*Incidence (%)*	*Tumor multiplicity/animal*	*Tumor range*	*Histology*	*Tumor localization*
$Smad4^{E6sad}$	6	8 months (6–12)	67	5	2–6	Hyperplastic polyps	S: 100%; P: 100%; D: 32%; J:55%; I: 23%; C: 12%
$Apc^{+/1638N}$	7	8 months (6–18)	100	4	1–10[a]	Low to high dysplastic polyps	S: 25%; P: 88%; D: 100%; J: 38%; I: 0%; C: 19%
TAS	8	7 months (3–8)	100	20	12–28[a]	Low to high dysplastic polyps; carcinomas	S: 100%; P: 100%; D: 100%; J: 87%; I: 37%; C: 0%
CAS	7	5 weeks (3–6)	100	60	22–88[a]	Low to high dysplastic polyps; microadenomas; carcinoma in situ	S: 25%; P: 100%; D: 100%; J: 100%; I: 42%; C: 0%

[a]$P<0.001$, Mann–Whitney rank sum test. Tumor localization: incidence of one or more lesions in the corresponding part of the intestinal tract: S = stomach, P = periampullar region, D = duodenum, J = jejunum, I = ileum, C = colon.

It is well established that constitutive activation of the Wnt/β-catenin signal transduction pathway, caused by either *Apc* or *Ctnnb1* (β-catenin) mutations, represents a rate-limiting event in intestinal tumor formation. β-Catenin nuclear accumulation is the hallmark of Wnt signaling activation and was analysed by IHC on tumor sections from $Smad4^{+/E6sad}$ mice. No β-catenin nuclear accumulation was observed in $Smad4^{+/E6sad}$ tumors, even at later stages of tumor development, thus indicating that Wnt signaling does not play a major role in *Smad4*-driven intestinal tumorigenesis (Figure 1f).

Tumor incidence and distribution in Trans *(TAS) and* Cis *(CAS)* $Apc^{+/1638N}/Smad4^{+/E6sad}$ *compound mutant mice*

To further investigate the role of the *Smad4* gene in GI tumor initiation and progression, we have bred $Smad4^{+/E6sad}$ mice with the $Apc^{+/1638N}$ mouse model, previously developed in our laboratory (Fodde *et al*., 1994). In the mouse genome, both the *Apc* and *Smad4* tumor suppressor genes are located on chromosome 18. Therefore, two different types of compound heterozygous mice were generated: *in Trans* $Apc^{+/1638N}/Smad4^{+/E6sad}$ (TAS), where the two mutations are present on two different chromosome 18 alleles, and *in Cis* $Apc^{+/1638N}/Smad4^{+/E6sad}$ (CAS), obtained by backcrossing TAS animals with C57BL/6 mice. In agreement with the genetic distance between the two tumor suppressor loci (33 cM), the two mutations were found on the same chromosome 18 allele in approximately 15% of the offspring.

The TAS and CAS mouse models showed distinctive phenotypes when compared to the single mutation littermates (Table 3) (Figure 4). For the present study, we analysed eight TAS (four female and four male subjects) and seven CAS (two female and five male subjects) mice.

The TAS lineage is characterized by a normal development, growth, and adult size. At age 6–7 months, mice present with an average of 20 tumors along the GI tract (range: 12–28), mainly in the duodenum. No neoplastic lesions were observed in the colon. The tumor multiplicity in TAS animals is significantly higher when compared to the $Apc^{+/1638N}$ and $Smad4^{+/E6sad}$ littermates ($P<0.001$, Mann–Whitney rank sum test) (Table 3). Histological analysis showed that the tumors were mainly villous or tubulovillous adenomas with foci of severe dysplasia and malignancy, similar to what has been observed in late stage $Apc^{+/1638N}$ tumors (Figure 3a). In two animals (age 6 and 7 months), adenocarcinomas with frank invasion of the muscolaris mucosa and submucosa were also observed (Figure 3b). All TAS mice also displayed desmoid tumors and cutaneous follicular cysts with similar incidence and distribution as previously observed in the $Apc^{+/1638N}$ mouse model (Smits *et al*., 1998). Owing to the high GI tumor multiplicity, TAS mice usually became moribund at around 7–8 months of age (Figure 4).

The CAS mouse model showed a more severe phenotype when compared with TAS. CAS mice became moribund at age 6 weeks; two out of nine CAS animals were found dead at 5 weeks and were not included in the analysis (Figure 4). Moribund mice were characterized by frank anemia and spleen enlargement. Macroscopic analysis of the intestinal tract revealed a very thin dystrophic intestinal wall and the presence of an average of 60 tumors per animal (range 22–88). Upon microscopic analysis, we observed numerous smaller lesions along the entire upper GI tract, previously referred to as GIN (gastrointestinal intraepithelial neoplasia) or microadenomas (Figure 3d) (Boivin *et al*., 2003). The polyps were either sessile or villous, and characterized by mild to severe dysplasia, in some cases with evident foci of malignant transformation, although no clear submucosal invasion was detected among 57 CAS tumors analysed here (Figure 3c).

LOH analysis of GI tumors from compound CAS and TAS $Apc^{+/1638N}/Smad4^{+/E6sad}$ *mice*

The LOH status at the *Apc* and *Smad4* loci was determined in 22 TAS and 16 CAS intestinal tumors. LOH analysis at the *Smad4* locus was carried out as

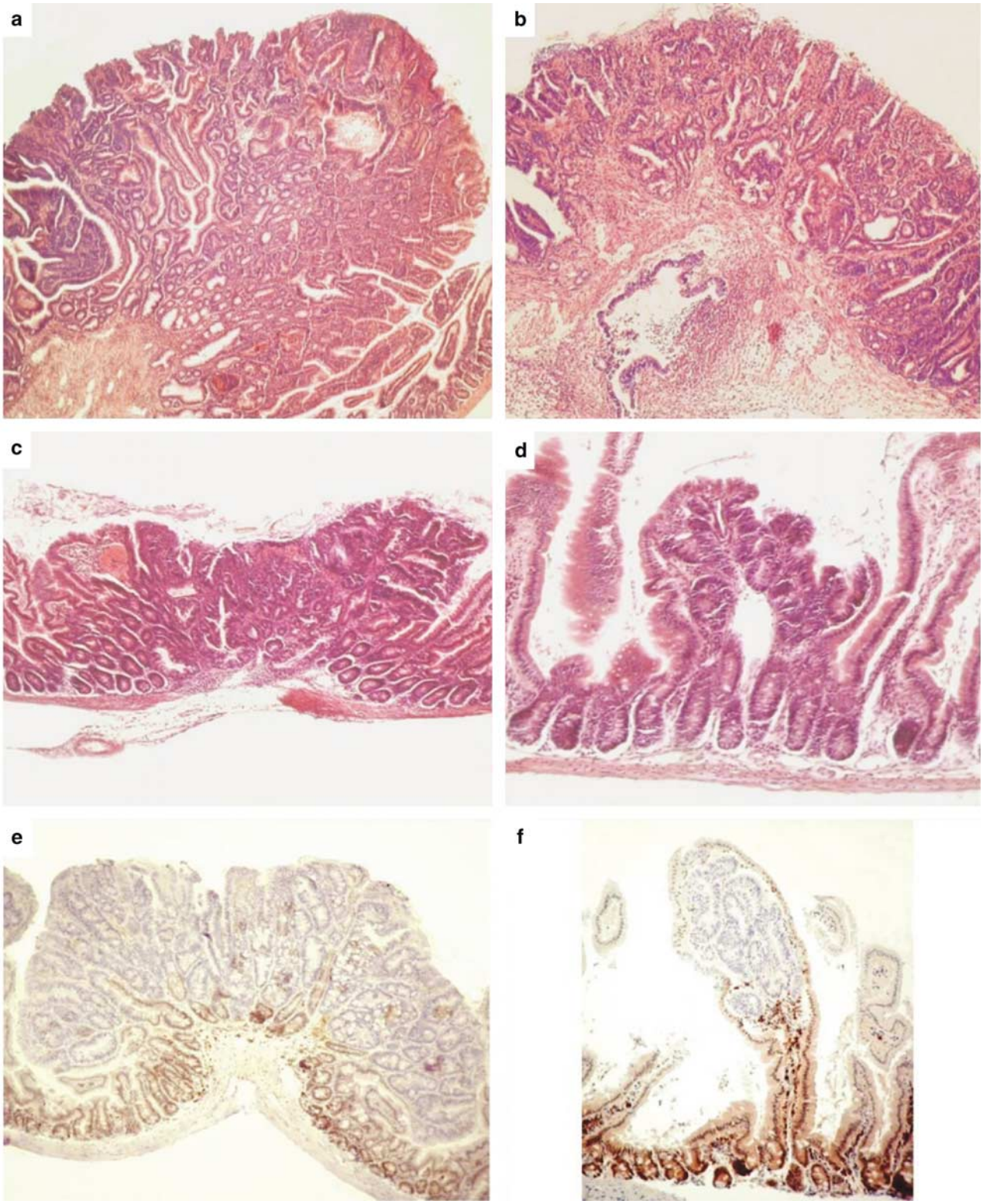

Figure 3 Histopathology and IHC analysis of intestinal tumors from compound $Apc^{+/1638N}/Smad4^{+/E6sad}$. (**a**) A typical dysplastic adenoma observed in TAS animals (HE staining). (**b**) An example of adenocarcinoma with extensive submucosal invasion from a TAS mouse (HE). (**c**) Sessile villous adenoma from a CAS mouse with areas of severe dysplasia and cystic formation (HE). (**d**) A nascent lesion or microadenoma observed in the duodenum of a CAS animal (HE). (**e**) Smad4 IHC analysis of a CAS tumor shows negative staining, thus indicating LOH of the wild-type allele. (**f**) Smad4 IHC analysis of a small microadenoma from the same CAS mouse also reveals LOH of the wild-type allele in the nascent lesion. Note the positively stained cells of the normal epithelial lining surrounding the dysplastic area.

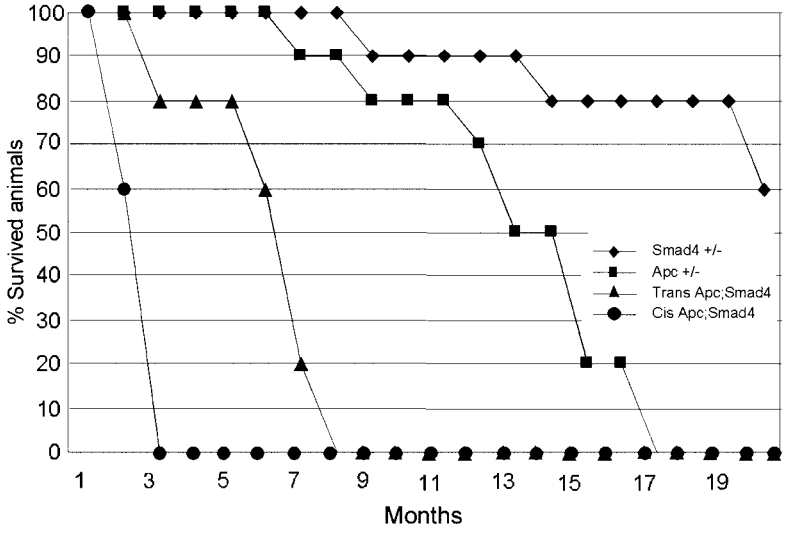

Figure 4 Survival plot of the different mouse models analysed in the present study.

Table 4 Smad4 LOH and IHC analysis of tumors from compound Apc^{1638N}/ $Smad4^{E6sad}$ (TAS and CAS) mice

Genotype	*No. of tumors*	*LOH wild-type Apc*	*LOH Smad4*	*Concomitant LOH*	*IHC SMAD4*
TAS	22	16/22 (73%)	10/22[a] (45%)	10/22 (45%)	+
CAS	16	11/16 (69%)	11/16[b] (69%)	7/16 (44%)	−

[a]Loss of *Smad4* ^{E6sad} mutant allele. [b]Loss of *Smad4* wild-type allele.

described above. For the *Apc* gene, tumor DNA was amplified with PCR primers specific for the wild-type and targeted Apc^{1638N} alleles (Smits *et al*., 1997).

Sixteen (73%) out of 22 TAS tumors showed LOH of the wild-type *Apc* allele, 10 of which (45%) with concomitant loss of the $Smad4^{E6sad}$ allele, as detected by the 2 cM distal flanking marker d18Mit80 (Table 4). Notably, none of the TAS tumors showed LOH at the wild-type *Smad4* allele. The LOH results were validated by direct sequencing of tumor DNA around the $Smad4^{E6sad}$ mutation site (exon 6 splice acceptor site). Sequence analysis confirmed in all cases (10/10) the results of the LOH analysis: where the loss of the $Smad4^{E6sad}$ allele was assessed by radioactive PCR, the frameshift, diagnostic for the presence of the mutation in the DNA from normal intestinal mucosa, was absent or strongly reduced in tumor samples (Figure 2d). In the remaining six tumors (27%), no LOH was detected at either loci, by either radioactive PCR and direct sequencing.

Among the CAS tumors, 11 (69%) out of 16 were characterized by LOH at the wild-type *Smad4* locus and the same percentage showed LOH at the wild-type *Apc* allele. In seven cases (44%), loss of both the *Apc* and Smad4 loci, and presumably of the entire chromosome 18, was observed. In only one CAS tumor, no LOH at either locus was detected (Table 4).

To confirm the above LOH results, Smad4 IHC analysis was performed on tumors from compound heterozygous $Apc^{+/1638N}$/$Smad4^{+/E6sad}$ mice. All TAS tumors analysed by IHC ($n=6$) showed positive staining for the Smad4 protein, thus confirming that LOH of the wild-type allele does not play a major role in tumor onset of this genetic combination. Unlike the TAS tumors, all CAS tumors analysed by IHC ($n=15$) were characterized by the complete absence of Smad4 staining, even at early stages of tumor formation, for example, the microadenomas (Figure 3e and f). The IHC data are in agreement with the LOH results obtained by DNA-based analysis where the majority of the tumors showed loss of wild-type *Smad4* and *Apc*, and presumably of the entire chromosome 18.

These results indicate that, although loss of Apc function seems to represent the rate-limiting event in tumor initiation in both types of compound $Apc^{+/1638N}$/ $Smad4^{+/E6sad}$ mice, the presence of LOH or haploinsufficiency at the *Smad4* gene differentially affects tumor initiation in the CAS and TAS genetic combinations.

Discussion

The *SMAD4* tumor suppressor gene has been shown to be inactivated in human colorectal cancer during late stages of the adenoma-carcinoma sequence (Takagi *et al*., 1996; Thiagalingam *et al*., 1996; Koyama *et al*., 1999; Miyaki *et al*., 1999). Owing to its relevance in GI tumor initiation and progression, and its central role in BMP/TGF-β signaling (Shioda *et al*., 1998; Itoh *et al*.,

2000; Fink *et al*., 2003), several investigators have generated *Smad4*-mutant mouse models to elucidate the mechanisms and the cellular consequences of its loss of function in intestinal cancer (Sirard *et al*., 1998; Takaku *et al*., 1999; Xu *et al*., 2000). In general, heterozygous $Smad4^{+/-}$ mouse models are predisposed to the development of multiple polyps of the upper GI tract, with variations in polyp numbers, histology, and onset, possibly due to differences in mutation type, for example, causing distinct defects in BMP/TGF-β signaling, and/or in genetic background. Among these, the $Smad4^{+/E6sad}$ mouse model has been previously reported and described by us as a model for serrated and hyperplastic adenoma due to a *null* mutation in the *Smad4* gene. In man, a consistent percentage of invasive colorectal carcinomas seems to originate from serrated and hyperplastic polyps (Jass, 2001; Makinen *et al*., 2001; Hawkins *et al*., 2002). From this perspective, the $Smad4^{+/E6sad}$ mouse is an interesting model to study alternative routes of intestinal carcinogenesis, other than the classic adenoma-carcinoma sequence.

In the present study, we first further characterized the phenotypic features of $Smad4^{+/E6sad}$ mice on an inbred C57BL6 genetic background, and investigated the mechanisms of somatic *Smad4* inactivation during GI tumor development and progression.

Onset of gastric and periampullary polyp formation occurs in $Smad4^{+/E6sad}$ mice between 6 and 9 months of age with 100% penetrance. Notably, penetrance of upper GI polyps was reported to be incomplete at around this age in other *Smad4* models (Takaku *et al*., 1999; Xu *et al*., 2000). $Smad4^{+/E6sad}$ mice were also affected by tumors in more distal locations along the intestine, namely in the duodenum, ileum, and in fewer cases in the colon. Also, unlike the *Smad4* model described by Xu *et al*. (2000), $Smad4^{+/E6sad}$ mice did not develop any carcinomas up to 18 months of age. Differences in the genetic background of the analysed mice may partly explain these discrepancies, as shown by the exclusive presence of gastric and periampullary tumors in the original F1 ($129 \times$ C57BL/6) $Smad4^{+/E6sad}$ animals (Hohenstein *et al*., 2003), whereas on the B6 background we also observed several tumors throughout the intestinal tract. However, differences in the molecular consequences of the targeted mutations may also underlie the phenotypic features of the individual models. In the case of the $Smad4^{E6sad}$ mutation, the splice acceptor mutation in exon 6 was shown by both RT–PCR and Western analysis to significantly affect mRNA stability and thus represent a *bona fide null* allele (Hohenstein *et al*., 2003). Unfortunately, similar molecular analyses were not reported for the other models which does not allow us to exclude that the above phenotypic differences are partly due to specific genotype–phenotype correlations at the *Smad4* locus (Takaku *et al*., 1999; Xu *et al*., 2000).

The histopathologic analysis of *Smad4* mutant tumors at different ages showed a slow but continuous progression from initial hyperplastic lesions to more advanced stages with clear dysplasia, similar to what has been observed in human CRC. In GI tumors from $Smad4^{+/E6sad}$ animals, LOH of the wild-type *Smad4* allele was only detected in advanced cases of tumor progression, with the majority of the tumors retaining heterozygosity in mice up to 12 months of age. IHC analysis with an antibody directed against the Smad4 protein confirmed that complete loss of Smad4 function is a late event in tumor progression, at first limited to more dysplastic areas of the neoplasms. These observations confirm the previous report by Xu *et al*. (2000), where tumors up to 0.4 cm in size were shown to retain the wild-type *Smad4* allele. Accordingly, somatic mutation analysis in cases of Familial Juvenile Polyposis (FJP) caused by *SMAD4* germline mutations showed LOH in only 9% (1/11) (Howe *et al*., 1998) and 23% (4/17) (Woodford-Richens *et al*., 2000) of the polyps, thus suggesting that a tumor suppressor gene dosage reduction, rather than its complete functional inactivation, characterizes the initial steps of *SMAD4*-driven GI tumor initiation and progression in mouse and man. We have previously shown that dosage variations in Wnt/β-catenin signaling differentially affect stem cell differentiation and multiorgan tumor predisposition in *Apc*-mutant mice (Gaspar and Fodde, 2004). Similarly, dosage fluctuations in BMP/TGF-β signaling in haploinsufficient *Smad4* intestinal cells may occasionally trigger epithelial hyperplasia either in combination with somatic mutations at genes other than *Smad4*, or due to gene dosage fluctuations under a putative BMP/TGF-β signaling threshold. In fact, impairment of BMP signaling may very well underlie tumor onset in $Smad4^{+/E6sad}$ mice, as inhibition of this pathway has been reported to result in the formation of numerous ectopic crypt units and frequent occurrence of intraepithelial neoplasia in mouse (Haramis *et al*., 2004). During tumor progression, complete loss of *Smad4* function blocks BMP and TGF-β signals from being transduced to the nucleus and is likely to underlie progression towards malignancy.

To further expand on the role of *Smad4* haploinsufficiency in intestinal tumor initiation and progression, and to study putative interaction between Wnt activation and BMP/TGF-β signaling impairment, we have bred $Smad4^{+/E6sad}$ animals with $Apc^{+/1638N}$, a mouse model previously developed in our laboratory, mainly characterized by tumors of the GI tract, desmoids, and epidermal tumors (Fodde *et al*., 1994; Smits *et al*., 1998). As both the *Apc* and *Smad4* genes are located on mouse chromosome 18, compound heterozygous $Apc^{+/1638N}$/$Smad4^{+/E6sad}$ mice were generated and studied in both the *in trans* (TAS) and *in cis* (CAS) genetic combinations. Both compound animals are characterized by an increase in tumor multiplicity, progression, morbidity, and mortality when compared to the single littermates. In CAS animals in particular, the presence of the two mutations on the same chromosome resulted in an extremely severe phenotype.

Notably, the compound heterozygotes generated in our study substantially differ from the $Dpc4^{+/-}$; $Apc^{\Delta 716+/-}$ *in trans* and *cis* models previously reported by Takaku *et al*. (1998). In this study, the *in trans* compound mice do not show phenotypic differences

when compared with the single $Apc^{+/\Delta 716}$ littermates. Also, the *in cis* compound mice are characterized by a decrease in polyp number and an increase in polyp size, with accelerated tumor progression and malignant transformation, still without affecting the survival.

The explanations for these phenotypic discrepancies may both reside in the difference in genetic background (B6 vs mixed 129/B6), and in the different molecular nature of the *Smad4*- and *Apc*-targeted mutations employed in the two studies. Indeed, the relatively mild intestinal tumor phenotype characteristic of $Apc^{+/1638N}$ mice is in sharp contrast with the severe morbidity of $Apc^{+/\Delta 716}$ animals with more than 500 GI tumors at 3 months of age. Also, the demonstrated hypomorphic nature of the Apc^{1638N} mutation encoding for residual β-catenin regulating activity (Smits *et al*., 1999; Kielman *et al*., 2002) is likely to differ from $Apc^{\Delta 716}$ resulting in a truncated Apc protein deprived of any β-catenin down-regulating activity with putative dominant-negative effects (Takaku *et al*., 1998). In the presence of such a highly penetrant *Apc* mutation, the *Smad4* mutation does not affect the tumor initiation event, whereas its effects are noticeable in the $Apc^{+/1638N}$ genetic background.

Loss of BMP signaling in CAS tumors upon loss of the *Smad4* wild-type allele can also contribute to the extremely severe phenotype observed in these mice. Notably, BMP signaling has been described to suppress Wnt signaling, ensuring a balance in the control of stem cell self-renewal (He *et al*., 2004). Loss of BMP-driven β-catenin regulation in CAS tumors may result in further enhancement of Wnt/β-catenin signaling to the nucleus and increased tumor formation.

An additional difference, although precise phenotypic comparisons between mouse strains in different animal facilities are not straightforward, consists in the apparently more severe intestinal tumor phenotype of $Smad4^{+/E6sad}$ mice in comparison with the targeted *Smad4* allele described by Takaku *et al*. (1998, 1999) (Hohenstein *et al*., 2003).

Here, we show that in both the TAS and CAS animals, approximately half (44%) of the tumors have concomitant LOH of the *Apc* and *Smad4* loci in the same chromosome, possibly as the result of homologous somatic recombination between homologs (Haigis and Dove, 2003). Notably, in TAS polyps, tumor formation is driven by the loss of wild-type *Apc* (73% of the tumors) rather than by the loss of the wild-type *Smad4* allele (none observed). Hence, LOH at the *Apc* locus is the rate-limiting event for tumor formation in TAS mice. However, *Smad4* haploinsufficiency clearly affects *Apc*-driven tumor initiation as indicated by the increased tumor multiplicity in TAS animals when compared with $Apc^{+/1638N}$. *Smad4* haploinsufficiency effects on *Apc*-driven tumor formation and progression can explain this result. First, as reported here and elsewhere, the observed *Smad4* haploinsufficiency in mouse and human polyps indicates that BMP/TGF-β signaling dosage fluctuations may contribute 'fertile soil' for polyp formation in the intestine. This may positively affect *Apc*-driven tumor formation both before and after the second hit at the wild-type *Apc* allele, possibly due to cumulative and/or synergistic effects of the concomitant signaling dosage defects. Accordingly, it has been shown that induction of TGF-β signaling in a nontransformed epithelial cell line reduces APC protein levels at the post-transcriptional level, and increases β-catenin mRNA and protein levels, causing its nuclear accumulation and transcriptional activation of Wnt downstream targets (Satterwhite and Neufeld, 2004). Wnt and TGF-β signaling may also cooperatively regulate a subset of downstream targets. Expression of the growth factor gastrin, a well-known Wnt target gene and GI-cancer promoter in mouse (Koh *et al*., 2000), is finely regulated by synergistic complexes of TGF-β/Smads and Wnt/β-catenin transcription factors (Lei *et al*., 2004).

In conclusion, our results confirm that *Smad4* haploinsufficiency is sufficient for intestinal tumor initiation and that loss of the wild-type allele underlies more advanced stages of tumor progression and dysplastic changes. More importantly, the analysis of the compound TAS and CAS mice has revealed a role for BMP/TGF-β signaling in *Apc*-driven tumor formation and possibly during progression towards malignancy. Reporter assay analysis of Wnt and BMP/TGF-β signaling activity in different genetic combinations and identification of the specific downstream targets will open the way for tailor-made therapeutic intervention.

Materials and methods

Mouse strains and tumor samples

All $Apc^{+/1638N}$ mice employed in this study were on an inbred C57BL/6Jico (B6) background. The employed $Smad4^{+/E6sad}$ mice were derived from F5-F8 backcross generations to C57BL/6 of the original F1 129Ola/C57BL/6Jico $Smad4^{+/E6sad}$ founder (Hohenstein *et al*., 2003). The in *Trans* $Apc^{+/1638N}/Smad4^{+/E6sad}$ (TAS) compound animals were generated by breeding $Smad4^{+/E6sad}$ with $Apc^{+/1638N}$ mice. The presence of both mutations in individual littermates is indicative of the TAS genotype.

The in *Cis* $Apc^{+/1638N}/Smad4^{+/E6sad}$ (CAS) model was obtained by backcrossing TAS animals with wild-type C57BL/6J mice. As both genes localize to the same chromosome 18, the presence of both mutations in individual littermates from TAS × C57BL/6J matings is indicative of a recombination event that has brought the mutant *Apc*- and *Smad4* alleles on the same chromosome 18. In agreement with the genetic distance between the two tumor suppressor loci (33 cM), the two mutations were found on the same chromosome 18 allele in approximately 15% of the offspring.

Tumors were obtained by macroscopic dissection of the GI tract and overnight fixation in Notox® (Earth Safe Industries, Inc., Bellemead, NJ, USA), as previous described (Smits *et al*., 1997), or after 4 h in 4% paraformaldehyde (PFA). Tumor sections were stained with hematoxylin and eosin (HE) and the histopathological analysis was performed using standard classification criteria (Boivin *et al*., 2003). The term polyp in this context was used to describe a macroscopic lesion that protrudes in the GI lumen. By histopathological analysis, the polyps were than defined as hyperplastic or

dysplastic-adenomatous polyps if they showed, respectively, gross thickening or proliferative dysplasia of the mucosa.

Laser capture microdissection and DNA extraction of intestinal tumors and normal mucosa

We employed laser capture microdissection (LCM) to obtain pure tumor cell populations from selected areas of paraffin-embedded tissue sections. In total, 10 μm Notox-fixed sections were deparaffinized, rehydrated, and briefly stained by HE. Consecutive sections were carefully microdissected using a PALM® MicroBeam microscope system (PALM Microlaser Technologies AG-Bernried, Germany). On average, 3000 cells were isolated from each designated area. For DNA isolation, LCM material was resuspended in 100 μl of extraction buffer (100 mM NaCl, 10 mM TrisHCl pH = 8.0, 25 mM EDTA pH = 8.0, 0.5% SDS) with 0.6 mg/ml Proteinase K, and incubated overnight at 60°C. After phenol/chloroform and chloroform extraction, DNA was precipitated for 30 min at −20°C with 200 μl of 100% ethanol, 50 μl 7.5 M NH4Ac, and 10 μg GenEluteTM linear polyacrylamide (Sigma), and suspended in 15 μl TE^{-4} buffer (10 mM Tris–HCl pH 8.0, 0.1 mM EDTA).

LOH analysis at the Apc *and* Smad4 *genes*

LOH analysis of the *Apc* gene was performed using three primers that amplify in a single PCR reaction both the wild-type and the targeted Apc^{1638N} allele, as previously described (Smits *et al*., 1997). LOH analysis of the *Smad4* gene was carried out by genotyping the microsatellite repeat markers d18Mit81 and d18Mit80, informative in the employed $Smad4^{+/E6sad}$ mice, located 7 and 2 cM, respectively, proximal and distal to the *Smad4* gene on chromosome 18. PCR products were resolved on 6% polyacrylamide gels and quantified using a Typhoon™ 9410 and ImageQuant™ TL (Molecular Dinamics). LOH was scored when the allelic ratio of the two bands, normalized for the average ratio of normal controls, was $\geqslant 1.5$ (Smits *et al*., 1997).

LOH analysis by sequence analysis

The following primer pair was employed to PCR amplify the $Smad4^{E6sad}$ mutation site within the intron5/exon6 boundary: *Smad4* F1-GGACAGCAGCAGAATGGATT and *Smad4* R1-ATGGCCGTTTTGGTGGTGAG.

PCR products were sequenced in both directions using the same primers. Sequencing was performed on an ABI 3700 capillary sequencer (Applied Biosystem, Foster City, CA, USA) according to the manufacturer's instructions.

Immunohistochemical analysis of Smad4 and β*-catenin*

Notox and PFA-fixed paraffin-embedded tumor sections (4 μm) were immunostained with mouse monoclonal antibodies direct against Smad4 (clone B-8, sc-7966, Santa Cruz Biotechnology, Santa Cruz, CA, USA; dilution 1:100) and β-catenin (Transduction Laboratories, clone 14; dilution 1:200). The specificity of the B-8 antibody has been previously tested and validated (Wilentz *et al*., 2000; Salovaara *et al*., 2002). After antigen retrieval treatment (10 min boiling in Tris-EDTA pH 8.0), endogenous peroxidases were inactivated by 1% H_2O_2/PBS. A preincubation step of 30 min in 5% nonfat dry milk in PBS was followed by incubation with the specific antibody overnight at 4°C in preincubation buffer. Sections were then incubated and stained with the Envision HRP-ChemMate kit (DAKO) for the Smad4 antibody, and with a goat antibody against mouse IgG/IgM conjugated with peroxidase (Jackson ImmunoResearch Laboratories) for β-catenin. The evaluation of Smad4 IHC staining was performed after brief hematoxylin counterstaining of the slides.

Acknowledgements

This work has been made possible by funds from the Dutch Cancer Society, the Dutch Research Council (NWO VICI), and BSIK (ICES/KIS-3). PH is supported by a grant from the Association for International cancer Research (AICR).

References

Boivin GP, Washington K, Yang K, Ward JM, Pretlow TP, Russell R *et al*. (2003). *Gastroenterology* **124**: 762–777.
Fearon ER, Vogelstein B. (1990). *Cell* **61**: 759–767.
Fink SP, Mikkola D, Willson JK, Markowitz S. (2003). *Oncogene* **22**: 1317–1323.
Fodde R, Edelmann W, Yang K, van Leeuwen C, Carlson C, Renault B *et al*. (1994). *Proc Natl Acad Sci USA* **91**: 8969–8973.
Gaspar C, Fodde R. (2004). *Int J Dev Biol* **48**: 377–386.
Haigis KM, Dove WF. (2003). *Nat Genet* **33**: 33–39.
Haramis AP, Begthel H, van den Born M, van Es J, Jonkheer S, Offerhaus GJ *et al*. (2004). *Science* **303**: 1684–1686.
Hawkins NJ, Bariol C, Ward RL. (2002). *Pathology* **34**: 548–555.
He XC, Zhang J, Tong WG, Tawfik O, Ross J, Scoville DH *et al*. (2004). *Nat Genet* **36**: 1117–1121.
Hohenstein P, Molenaar L, Elsinga J, Morreau H, van der Klift H, Struijk A *et al*. (2003). *Genes Chromosomes Cancer* **36**: 273–282.
Howe JR, Roth S, Ringold JC, Summers RW, Jarvinen HJ, Sistonen P *et al*. (1998). *Science* **280**: 1086–1088.
Itoh S, Itoh F, Goumans MJ, Ten Dijke P. (2000). *Eur J Biochem* **267**: 6954–6967.
Jass JR. (2001). *J Pathol* **193**: 283–285.
Kielman MF, Rindapaa M, Gaspar C, van Poppel N, Breukel C, van Leeuwen S *et al*. (2002). *Nat Genet* **32**: 594–605.
Koh TJ, Bulitta CJ, Fleming JV, Dockray GJ, Varro A, Wang TC. (2000). *J Clin Invest* **106**: 533–539.
Koyama M, Ito M, Nagai H, Emi M, Moriyama Y. (1999). *Mutat Res* **406**: 71–77.
Lei S, Dubeykovskiy A, Chakladar A, Wojtukiewicz L, Wang TC. (2004). *J Biol Chem* **279**: 42492–42502.
Makinen MJ, George SM, Jernvall P, Makela J, Vihko P, Karttunen TJ. (2001). *J Pathol* **193**: 286–294.
Miyaki M, Iijima T, Konishi M, Sakai K, Ishii A, Yasuno M *et al*. (1999). *Oncogene* **18**: 3098–3103.
Salovaara R, Roth S, Loukola A, Launonen V, Sistonen P, Avizienyte E *et al*. (2002). *Gut* **51**: 56–59.
Satterwhite DJ, Neufeld KL. (2004). *Cell Cycle* **3**: 1069–1073.
Shioda T, Lechleider RJ, Dunwoodie SL, Li H, Yahata T, de Caestecker MP *et al*. (1998). *Proc Natl Acad Sci USA* **95**: 9785–9790.
Sirard C, de la Pompa JL, Elia A, Itie A, Mirtsos C, Cheung A *et al*. (1998). *Genes Dev* **12**: 107–119.
Smits R, Kartheuser A, Jagmohan-Changur S, Leblanc V, Breukel C, de Vries A *et al*. (1997). *Carcinogenesis* **18**: 321–327.
Smits R, Kielman MF, Breukel C, Zurcher C, Neufeld K, Jagmohan-Changur S *et al*. (1999). *Genes Dev* **13**: 1309–1321.

Smits R, van der Houven van Oordt W, Luz A, Zurcher C, Jagmohan-Changur S, Breukel C *et al*. (1998). *Gastroenterology* **114**: 275–283.

Takagi Y, Kohmura H, Futamura M, Kida H, Tanemura H, Shimokawa K *et al*. (1996). *Gastroenterology* **111**: 1369–1372.

Takaku K, Miyoshi H, Matsunaga A, Oshima M, Sasaki N, Taketo MM. (1999). *Cancer Res* **59**: 6113–6117.

Takaku K, Oshima M, Miyoshi H, Matsui M, Seldin MF, Taketo MM. (1998). *Cell* **92**: 645–656.

Thiagalingam S, Lengauer C, Leach FS, Schutte M, Hahn SA, Overhauser J *et al*. (1996). *Nat Genet* **13**: 343–346.

Wilentz RE, Su GH, Dai JL, Sparks AB, Argani P, Sohn TA *et al*. (2000). *Am J Pathol* **156**: 37–43.

Woodford-Richens K, Williamson J, Bevan S, Young J, Leggett B, Frayling I *et al*. (2000). *Cancer Res* **60**: 2477–2482.

Xu X, Brodie SG, Yang X, Im YH, Parks WT, Chen L *et al*. (2000). *Oncogene* **19**: 1868–1874.